Typeset version here: https://doi.org/10.1016/j.precamres.2020.105729

Please cite as:
Staude, S., Jones, T.J. and Markl, G., 2020. The textures, formation and dynamics of rare high-MgO komatiite pillow lavas. *Precambrian Research*, *343*, p.105729.

Typeset version here: https://doi.org/10.1016/j.precamres.2020.105729

The textures, formation and dynamics of rare high-MgO komatiite pillow lavas

Sebastian Staude[1], Thomas J. Jones[2], Gregor Markl[1]

[1]*Department of Geosciences, University of Tübingen, Wilhelmstraße 56, D-72074 Tübingen, Germany*

[2]*Department of Earth, Environmental and Planetary Sciences, Rice University, 6100 Main Street, Houston, TX 77005, USA*

Corresponding author: Sebastian Staude – Sebastian.staude@uni-tuebingen.de

Typeset version here: https://doi.org/10.1016/j.precamres.2020.105729

Abstract

Pillow lavas are an abundant morphological lava type both on Earth and on some extraterrestrial bodies. We examine pillows from Kambalda (Western Australia) komatiites, that uniquely preserve pillow necks, inter-pillow cavities, and internal crusts. Our study is the first description of true pillows from an Archaean high-MgO (~ 31%) komatiite. Their size ranges from 0.5 to 5 cm and most have equal vertical and horizontal axes. Due to very low melt viscosities (~0.01 – 0.1 Pa s), these komatiite pillows are one to two orders of magnitude smaller than modern basaltic counterparts. True high-MgO komatiites, such as those at Kambalda, require a low flow rate, potentially found on distal flow edges. Such low flow rates are in conflict with the high flow velocities generally assumed for komatiites, and hence explains the rarity of komatiite pillow lavas.

Keywords

komatiite; Kambalda; pillow lava; Archaean; lava viscosity; lava morphology

Typeset version here: https://doi.org/10.1016/j.precamres.2020.105729

1. Introduction

Komatiites (>18 wt. % MgO) and komatiitic basalts (<18 wt. % MgO) are ultramafic magmatic rocks which are mostly restricted to the Archean and Precambrian. Therefore, they provide crucial information about Earth's early history and evolution (Huppert et al., 1984; Canil, 1997; Bekker et al., 2009). Komatiites erupted with temperatures several hundreds of degrees higher than present-day basaltic lavas. This and their ultramafic composition gave rise to extremely low melt viscosities and unique emplacement conditions. Such phenomena include extensive thermal erosion (10s of meters) of the underlying substrate and meter-sized skeletal crystals (called spinifex) located on lava flow tops reflecting high cooling rates and large degrees of undercooling (e.g. Huppert et al., 1984; Nisbet et al., 1993; Arndt et al., 2008; Staude et al., 2016). Furthermore, komatiite-related Ni sulfide deposits are of great economic interest (Arndt et al., 2008). Extra-terrestrial occurrences have been observed during eruption (on Jupiter's moon Io; Williams et al., 2000) and hence the analogy to the Archean examples can provide critical information about dynamic processes on other planets and moons (e.g. Leverington, 2018).

Pillow lavas are an abundant product of mafic volcanism and commonly form during subglacial and subaqueous lava extrusion or lava entry into wet sediments (e.g. Walker, 1992; Moore, 1975; Jones, 1968; Yamagishi, 1985). Thus, the simple presence and morphological features of pillow lavas can be used to constrain both paleoenvironment and eruption conditions (Jones, 1969; Fridleifsson et al., 1982; Walker, 1992; Gregg and Fink, 1995). Pillow lavas in komatiitic basalts have been reported from several locations and tend to be smaller than their basaltic counterparts (Barberton, South Africa, Smith et al., 1984; Kuhmo, Finland, Hanski, 1980; Abitibi, Dostal and Mueller, 1997). In contrast, pillowed lava flows in true komatiites (e.g. MgO >18 wt. %, olivine as liquidus phase) are extremely rare and have been reported at only a

few locations. A description of komatiite pillows from the Belingwe Greenstone Belt (Zimbabwe; Nisbet et al., 1977; 1993) report komatiites with 26 wt.% volatile-free MgO having pillows with 20-50 cm diameter and a 2 cm thick crust. Dostal and Mueller (1997) report komatiite pillows and pillow tubes to be 10-50 m (probably a typographical error; their photos show pillows of 10-50 cm diameter) from a komatiite at Abitibi (Canada) which they report to have around 23% MgO. Similarly, Hanski (1980) reports low-MgO komatiite (19-22 % MgO) pillows from Kuhmo (Finland) with sizes of 0.1 to 1 m. All these pillow descriptions are incomplete and/or lack key details. This and their geochemical composition raise doubts as to whether they represent true pillow lava (Arndt et al., 2008).

Furthermore, Arndt et al. (2008) distinguished two types of pillow-like structures in komatiites: firstly, 0.5 m to 6 m wide and 0.3 m to 2 m high lobes which partly display spinifex-textures in the upper portion. They are interpreted as the initial lobes of the advancing lava flow similar to those observed in an advancing pahoehoe flow. Secondly, 0.2 m to 1 m spherical structures within olivine porphyritic komatiite of unclear origin could represent polyhedral joints (Arndt et al., 2008). Arndt et al. (2008) also stated that pillows are common in komatiitic basalts, occasionally in low-MgO komatiites, and unknown in high-MgO komatiites.

All the previously described occurrences of (potential) komatiite pillows are from low-MgO komatiites. Here we present the first detailed description of high-MgO komatiite pillows that are uniquely preserved in Kambalda (Western Australia). We document their internal flow textures and quantify their morphology. We compare komatiite pillow size to other pillow lavas from the literature to reveal a viscosity-size relationship that spans a wide range in silica content, from ultramafic to intermediate compositions.

Typeset version here: https://doi.org/10.1016/j.precamres.2020.105729

2. Occurrence of komatiite pillow lavas

The 2.7 Ga old Kambalda komatiite is part of the Kalgoorlie Terrane of the Yilgarn Craton (Fig. 1; Gresham and Loftus-Hills, 1981; Goscombe et al., 2009). Despite an upper greenschist facies metamorphic overprint, many igneous and sedimentary textures are nicely preserved in the Kambalda sequence (Gresham and Loftus-Hills, 1981; Staude et al., 2016; 2017a; *in press*) and hence the prefix 'meta' is omitted in the literature. The tholeiitic Lunnon basalt is the basal unit and is overlain by <5 m thick chlorite- and chert-rich sediments (Gresham and Loftus-Hills, 1981) which are followed by the Silver Lake komatiite that also hosts chert-rich sedimentary layers (Fig. 1). The chlorite-rich sediments represent the relicts of erosion of the underlying lava flow, whereas the cherts have a chemical and volcaniclastic origin (Beresford and Cas, 2001).

The Silver Lake komatiite is split into a thin differentiated flow facies and a channelized compound sheet flow facies (Gole and Barnes, 2020). Thin differentiated flows are usually <5 m thick and form spinifex and cumulate textured flows with multiple units reaching several hundred meters of total thickness (Gole and Barnes, 2020). In channelized flows, which can be up to 150 m thick, komatiite and sulfide melt eroded the underlying sediments and basalt to form the Ni sulfide deposits of Kambalda (Huppert and Sparks, 1985; Staude et al., 2016, 2017a, 2017b). The parental magma of the komatiite is reported to have 31 wt.% MgO (Arndt et al., 2008, and references therein). The Silver Lake komatiite is followed, in stratigraphic sequence, by the Tripod Hill komatiite and younger volcanic and sedimentary rocks (Gresham and Loftus-Hills, 1981).

The observed pillow lavas in the Silver Lake komatiite documented here are found ~ 40 m above the basalt-komatiite contact and occur in four horizons, extending up to 1 m in

thickness within a 10 m thick interval between the Lunnon and McLeay deposits (drill hole DDH065-W2; Fig. 1). The pillow lava horizons overlie spinifex-textured or vesicular komatiite. The pillows shown in Figures 2 and 3 are part of the same pillowed flow. The lower contact of vesicular to pillowed komatiite is approximately 30-40° steeper with respect to the regional stratigraphy and the upper contact with a 1.5 m thick random spinifex-textured komatiite, is approximately 20° steeper. However, it is unclear whether the spinifex-textured komatiite which is followed by pillowed komatiite above, intruded as a sill or is stratiform. Neighboring drill holes do not display pillows. At the same stratigraphic level, the drill hole to the west (DDH065-W3) contains sediments, whereas in the one to the east (DDH065-W4) lacks a characteristic komatiite texture and sediments are absent (Fig. 1).

3. Morphological and textural features

The pillows observed in the drill core range in size from 0.5 to 5 cm (electronic supplementary material (ESM) 1). They have equal vertical to horizontal axes apart from the larger pillows (>2 cm), which show width to height ratios of up to 0.3. The crust ranges between 1 and 6 mm in thickness and, in some cases, necks are preserved between connected pillow lobes (Fig. 2) as well as inter-pillow cavities (Figs. 2 and 3). Microscopically, the pillows consist of fine-grained talc, chlorite, carbonate and magnetite, whereas the inter-pillow space is composed of talc and carbonate only. Magnetite is very abundant in the crust of the pillow (about 3-5 vol.% compared to <1 % within the pillow), and, in some cases, highlights multiple internal crusts within a pillow, which could be interpreted as recharging and inflation by another melt pulse (Fig. 4). In the center of some larger pillows (> 2 cm), an assemblage of magnetite-free, fine-grained talc±chlorite pseudomorphs euhedral crystals, most likely olivine. Between these

euhedral crystals, magnetite forms elongate aggregates, reflecting skeletal crystals - probably spinifex-textured olivine.

The inter-pillow space is composed of talc and carbonate which is a typical metamorphic product of komatiite at Kambalda (Gresham and Loftus-Hills, 1981). It is unclear whether these minerals replace something else or fill empty void space. Squire et al. (1998) reported quartz, carbonate, epidote and garnet to fill the inter-pillow space in the Lunnon basalt. This is also a typical metamorphic assemblage and Squire et al. (1998) only state that it is a post-depositional feature.

4. Comparison to pillow lavas of other composition

Lava (erupted in contact with water/ice) can exist in a wide range of morphologies such as sheet-like flows, lobes and pillows (e.g. Fox et al., 1987; Gregg and Fink, 1995). This has been attributed to eruption conditions (e.g. effusion rate), environmental conditions (e.g. substrate type and slope) and the lava properties (e.g. temperature, composition, crystal content), where the latter essentially leads to variations in lava rheology (Ballard et al., 1979; Luyendyk and Macdonald, 1985; Bonatti and Harrison, 1988; Gregg and Fink, 1995; McClinton and White, 2015; Rader et al., 2017; Maschmeyer et al., 2019). Laboratory studies of lava morphology have provided quantitative insight into the conditions of formation (Griffiths and Fink, 1992; Gregg and Fink, 1995). It was found that lavas evolve from sheets to lobes to pillows due to an increase in their cooling rate, a decrease in the substrate slope and a decrease in their flow rate. For a specified substrate slope and cooling rate, higher lava viscosities and lower flow rates favor pillow formation. Specifically, at sufficient cooling rates Gregg and Fink (1995) calculated that lava on a 10° slope with a viscosity of ~ 15 Pa s requires point source flow rates $< 10^{-3}$ m^3 s^{-1}.

This framework explains the rarity of komatiite pillow lavas. Given the low viscosities (0.1-10 Pa s) predicted for komatiite lavas (Huppert and Sparks, 1985) and the high estimated effusion/eruption rates (0.5-100 m^2 s^{-1} per unit width of flow; Huppert and Sparks, 1985), we contend that 'true' pillow formation in komatiites is rare and larger 'pillow-like' structures previously observed are likely representative of tube feeder systems (Arndt et al., 2008). We hypothesize that the pillows observed in Kambalda formed at the edge of a flow unit where the local flow rate was low and where water was available to provide an increased cooling rate.

A comprehensive catalogue of the geometry of pillow lavas (particularly their heights and widths) as function of lava composition (e.g. olivine tholeiite, andesite) was provided by Walker (1992). The geometry of pillow lavas depends on a series of factors such as lava composition (i.e. viscosity), local topography and lava supply rate. It is also useful to note that similar, but not identical, factors are important during the formation and growth of Pahoehoe lobes (Crown and Baloga, 1999; Miyamoto and Crown, 2006). For pillow lavas, Walker (1992) concluded that the size dependence of pillows is controlled mainly by lava viscosity, the other factors only providing a second order control.

To test and extend these previous morphological studies, we measured the height and width of the Silver Lake komatiite pillows (ESM 1). As our observations were made on drill cores, our measurement technique differs slightly from the one used by Walker (1992). However, our measurements represent the longest and the perpendicular dimension, which was always the shortest and, hence, represent approximately the true dimensions. Then, to provide a quantitative estimate of pillow lava viscosity, powder XRF data (ESM 2) of the pillow and adjacent spinifex-textured komatiite Fig. 3; ESM 3) as well as bulk chemistry measurements for the Silver Lake komatiite (Staude and Markl, 2019) were used to compute the melt viscosity (Giordano et al.,

2008). The MgO content of the pillow was recalculated to account for the volatiles; MgO is 31.2% in the pillow and 30.5% in the adjacent spinifex-textured flow. For comparison, the dimensions of other pillow lavas with different composition were taken from the literature (Fig. 5). We computed the melt viscosity following Giordano et al. (2008), but we note that in the absence of glass chemical data (representing the true melt), bulk rock data were used as the best approximation (Fridleifsson et al., 1982; Bear and Cas, 2007; Nisbet et al., 1977; 1993; Hanski 1980). Our data compilation (ESM 4) shows that komatiite pillow lavas perfectly follow and augment the viscosity-size spectrum, further supporting the notion that, to a first order, pillow size is controlled by lava viscosity. This further supports our hypothesis that the large (several decimeters to meters) 'pillows' previously observed in komatiite lavas (Arndt et al., 2008, and references therein) are likely feeder systems rather than true pillow lavas.

The validity of using chemical data from an altered rock containing only secondary minerals is supported by a number of previous studies. These have shown that Mg, Fe, Mn, and Al are all relatively immobile during the seafloor alteration and regional metamorphism observed at Kambalda (Lesher and Arndt, 1995, and references therein). Calcium and Si are slightly to strongly mobile (particularly in cumulates), and K and Na are highly mobile (Lesher and Arndt, 1995, and references therein). Although the pillowed komatiite contains talc, chlorite and carbonates, its geochemical composition (ESM 2) is similar to other MgO-rich komatiite reported from Kambalda and other greenstone belts (Arndt et al., 2008, and references therein). The melt composition is only one factor of uncertainty in the viscosity calculations, others include the melt temperature and the suspended bubble and crystal content. Thus, we present the viscosity estimates with a large 300°C temperature variation to reflect such uncertainties and we stress that these viscosity estimates serve as points of comparison, not exact values. Furthermore,

196 the viscosity range reported here, is in agreement with previously published viscosities for
197 Kambalda komatiite (Williams et al., 2000).
198
199 **5. Implications and summary**
200 The preservation of delicate spinifex textures within the pillows and surrounding
201 komatiite (including the amygdales) shows that this texture represents true high-MgO komatiite
202 pillows despite the talc-carbonate overprint usually destroying igneous textures (Arndt et al.,
203 2008). Their three-dimensional shape is visible in the cylindrical drill core; hence they can be
204 classified as pillows and not as lava lobe fronts which would result in fingers rather than three-
205 dimensional isolated pillows. The pillow necks, pinch offs and inter-pillow cavities further
206 document the dynamic process forming these pillows. Therefore, we document for the first time,
207 true high-MgO (~ 31%) komatiite pillows and show that they are in the centimeter rather than
208 decimeter or meter scale as previously reported.
209 The pillows most likely formed on the edge of a flow unit where the local flow rate was
210 low. This is further supported by the drill profiles (Fig. 1). The western drill hole shows chert
211 and the eastern drill hole massive komatiite at the same stratigraphic level. Additionally,
212 different lithology contact angles were observed underneath and above the pillow horizon.
213 Interestingly, below the chert is a vesicular horizon which is also observed below the basal
214 pillow komatiite (ESM 3). As the pillow deposits show evidence of dynamic features such as
215 break outs and refilling, the formation conditions are likely comparable to other, well
216 documented, mafic volcanic rocks (e.g. basalts) and only differ in their size. Hence, the pillow
217 size shows a continuum from komatiites to komatiitic basalt to basalt to andesite (Fig. 5), which
218 is largely controlled by the melt viscosity. This further extends the data provided by Walker

Typeset version here: https://doi.org/10.1016/j.precamres.2020.105729

(1992). We contend that 'true' pillows are rare in komatiites as a low local flow rate is required, which is in conflict with the high eruption rates and low viscosities thought to characterize komatiite.

Acknowledgments

We are grateful to IGO for providing the drill hole samples. Two anonymous reviewers are thanked for their fast and thorough review of the manuscript. The research was funded by the German Research Foundation (grant number: 407352165) to SS. TJJ acknowledges support from a Rice Academy Fellowship.

Typeset version here: https://doi.org/10.1016/j.precamres.2020.105729

References

Arndt, N.T., Lesher, C.M., Barnes, S.J., 2008. Komatiite. Cambridge University Press, New York.

Ballard, R.D., Holcomb, R.T. van Andel, T.H., 1979. The Galapagos Rift at 86°W: 3. Sheet flows, collapse pits and lava lakes of the rift valley. J. Geophys. Res. 84, 5407–5422.

Bear, A.N., Cas, R.A.F., 2007. The complex facies architecture and emplacement sequence of a Miocene submarine mega-pillow lava flow system, Muriwai, North Island, New Zealand. J. Volcanol. Geoth. Res. 160, 1-22.

Bekker, A., Barley, M.E., Fiorentini, M.L., Rouxel, O.J., Douglas, R., Beresford, S.W., 2009. Atmospheric sulfur in Archean komatiite-hosted nickel deposits. Sc. 326, 1086-1089.

Beresford, S.W., Cas, R.A.F., 2001. Komatiitic invasive lava flows, Kambalda, Western Australia. Can. Mineral. 39, 525-535.

Bonatti, E., Harrison, C.G.A., 1988. Eruption styles of basalt in oceanic spreading ridges and seamounts: Effect of magma temperature and viscosity. J. Geophys. Res. 93, 2967–2980.

Canil, D., 1997. Vanadium partitioning and the oxidation state of the Archaean komatiite magmas. Nature 389, 842-845.

Crown, D.A., Baloga, S.M., 1999. Pahoehoe toe dimensions, morphology, and branching relationships at Mauna Ulu, Kilauea Volcano, Hawai'i. Bull. Volcanol. 61, 288-305.

Dostal, J., Mueller, W.U., 1997. Komatiite flooding of a rifted Archean rhyolitic arc complex: geochemical signature and tectonic significance of the Stoughton-Roqeumaure Group, Abitibi Greenstone belt, Canada. J. Geol. 105, 545-564.

Fox, C.G., Murphy, K.M., Embley, R.W., 1987. Automated display and statistical analysis of interpreted deep-sea bottom photographs. Mar. Geol. 78, 199–216.

Typeset version here: https://doi.org/10.1016/j.precamres.2020.105729

253 Fridleifsson, I.B., Furnes, H., Atkins, F.B., 1982. Subglacial volcanics—on the control of magma
254 chemistry on pillow dimensions. J. Volcanol. Geoth. Res. 13, 103-117.
255 Giordano, D., Russell, J.K., Dingwell, D.B., 2008. Viscosity of magmatic liquids: a model. Earth
256 Planet. Sc. Lett. 27, 123-134.
257 Gole, M.J., Barnes, S.J., 2020. The association between Ni-Cu-PGE sulfide and Ni-Co lateritic
258 ores and volcanic facies within the komatiites of the 2.7 Ga East Yilgarn Craton Large Igneous
259 Province, Western Australia. Ore Geol. Rev. 116, 103231.
260 Goscombe, B., Blewett, R.S., Czarnota, K., Groenwald, P.B., Maas, R., 2009. Metamorphic
261 evolution and integrated terrane analysis of the Eastern Yilgarn Craton: rationale, methods,
262 outcomes and interpretation. Geosc. Austral. Rec. 2009/23.
263 Gregg, T.K., Fink, J.H., 1995. Quantification of submarine lava-flow morphology through
264 analog experiments. Geol. 23, 73-76.
265 Gresham, J.J., Loftus-Hills, G.D., 1981. The geology of the Kambalda nickel field, Western
266 Australia. Econ. Geol. 76, 1373-1416.
267 Griffiths, R.W., Fink, J.H., 1992. Solidification and morphology of submarine lavas: A
268 dependence on extrusion rate. J. Geophys. Res. 97, 19,729–19,737.
269 Hanski, E., 1980. Komatiitic and tholeiitic metavolcanics of the Siivikkovaara area in the
270 Archean Kuhmo greenstone belt, Eastern Finland. Bull. Geol. Soc. Finland 52, 67-100.
271 Huppert, H.E., Sparks, R.S.J., Turner, J.S., Arndt, N.T., 1984. Emplacement and cooling of
272 komatiite lavas. Nat. 309, 19-22.
273 Huppert, H.E., Sparks, R.S.J., 1985. Komatiites I: Eruption and flow. J. Petrol. 26, 694-725.
274 Jones, J.G., 1969. Pillow lavas as depth indicators. Am. J. Sc. 267, 181-195.
275 Jones, J.G., 1969. Pillow lavas as depth indicators. Am. J. Sc. 267, 181-195.

Typeset version here: https://doi.org/10.1016/j.precamres.2020.105729

276 Lesher, C.M., Arndt, N.T., 1995. REE and Nd isotope geochemistry, petrogenesis and volcanic
277 evolution of contaminated komatiites at Kambalda, Western Australia. Lith. 34, 127-157.
278 Leverington, D.W., 2018. Is Kasei Valles (Mars) the largest volcanic channel in the solar
279 system?. Icarus 301, 37-57.
280 Luyendyk, B.P., Macdonald, K.C., 1985. A geological transect across the crest of the East
281 Pacific Rise at 21°N latitude made from the deep submersible ALVIN. Mar. Geophys. Res. 7,
282 467–488.
283 Maschmeyer, C.H., White, S.M., Dreyer, B.M., Clague, D.A., 2019. High-Silica Lava
284 Morphology at Ocean Spreading Ridges: Machine-Learning Seafloor Classification at Alarcon
285 Rise. Geosc. 9, 245.
286 McClinton, J.T., White, S.M., 2015. Emplacement of submarine lava flow fields: A
287 geomorphological model from the Niños eruption at the Galápagos Spreading Center. Geochem.
288 Geophys. Geosyst. 16, 899-911.
289 Miyamoto, H., Crown, D.A., 2006. A simplified two-component model for the lateral growth of
290 pahoehoe lobes. J. Volcanol. Geoth. Res. 157, 331-342.
291 Moore, J.G., 1975. Mechanism of formation of pillow lava. Am. Sc. 63, 269-277.
292 Nisbet, E.G., Bickle, M.J., Martin, A., 1977. The mafic and ultramafic lavas of the Belingwe
293 Greenstone Belt, Rhodesia. J. Petrol. 18, 521-566.
294 Nisbet, E.G., Cheadle, M.J., Arndt, N.T., Bickle, M.J., 1993. Constraining the potential
295 temperature of the Archaean mantle: A review of the evidence from komatiites. Lith. 30, 291-
296 307.
297 Rader, E., Vanderkluysen, L., Clarke, A., 2017. The role of unsteady effusion rates on inflation
298 in long-lived lava flow fields. Earth Planet. Sc. Lett. 477, 73-83.

299 Smith, H.S., O'Neill, J.R., Erlank, A.J., 1984. Oxygen isotope compositions of minerals and
300 rocks and chemical alteration patterns in pillow lavas from the Baberton Greenstone Belt, South
301 Africa, in: Kröner, A., Hanson, G.N., Goodwin, A.M. (Eds.), Archean Geochemistr. Springer,
302 pp. 115-137.
303 Squire, R.J., Cas, R.A.F., Clout, J.M.F., Behets, R., 1998. Volcanology of the Archaean Lunnon
304 Basalt and its relevance to nickel sulfide-bearing trough structures at Kambalda, Western
305 Australia. Austral. JourJ. Earth Sc. 45, 695-715.
306 Staude, S., Barnes, S.J., Le Vaillant, M., 2016. Evidence of lateral thermomechanical erosion of
307 basalt by Fe-Ni-Cu sulfide melt at Kambalda, Western Australia. Geol. 44, 1047-1050.
308 Staude, S., Barnes, S.J., Le Vaillant, M., 2017a. Thermomechanical erosion of ore-hosting
309 embayments beneath komatiite lava channels: textural evidence from Kambalda, Western
310 Australia. Ore Geol. Rev. 90, 446-464.
311 Staude, S., Sheppard, S., Parker, P., Paggi, J., 2017b. Long-Victor nickel sulphide complex,
312 Kambalda, Western Australia, in: Phillips, N. (Ed.), Australian ore deposits, Monograph 32, 107-
313 112.
314 Staude, S., Markl, G., 2019. Remnant lenses of komatiitic dykes in Kambalda (Western
315 Australia): Occurrences, textural variations, emplacement model, and implications for other
316 komatiite provinces. Lith. 342-343, 206-222.
317 Staude, S., Barnes, S.J., Markl, G., in press. Interspinifex Ni sulfide ore from Victor South-
318 McLeay, Kambalda, Western Australia. Mineralium Deposita.
319 Walker, G.P.L., 1992. Morphometric study of pillow-size spectrum among pillow lavas. Bull.
320 Volcanol. 54, 459-474.
321 Williams, D.A., Wilson, A.H., Greeley, R., 2000. A komatiite analog to potential ultramafic

Typeset version here: https://doi.org/10.1016/j.precamres.2020.105729

materials on Io. J. Geophys. Res. 105, 1671-1684.

Yamagishi, H., 1985. Growth of pillow lobes—evidence from pillow lavas of Hokkaido, Japan, and North Island, New Zealand. Geol. 13, 499-502.

Typeset version here: https://doi.org/10.1016/j.precamres.2020.105729

Figure Captions

Figure 1. Simplified geology with the bottom left inset showing the study location in SW Australia. (A) Cross section through the Silver Lake komatiite where pillowed komatiite was drilled. Pillowed komatiite is only intersected in one drill hole (DDH065-W2) with sediments at the same stratigraphic level to the west (DDH065-W3) and sediment-free komatiite to the east (DDH065-W4). Lithology intersected along drill path are color-coded (see legend). Komatiite flow-direction was most likely NW to SE, based on sulfide ore situated on preserved sedimentary rocks being more common in the SE of the Kambalda district (Staude et al., 2017b). (B) Simplified geology of Kambalda with the collar location (red square) of drill holes DDH065. Numbers are: 1-Lunnon deposit, 2-McLeay deposit.

Figure 2. Pillow textural features and interpreted dynamic processes in drill core DDH065-W2, located at the base of the pillowed komatiite unit intersected which is overlying vesicular komatiite. (A) A series of merged photographs of a cylindrical drill core that contains pillowed komatiite. A sketch of the image is shown in (B). A neck between two pillows indicates the flow direction. Vesicles and inter-pillow spaces are filled by a white talc-carbonate assemblage.

Figure 3. Pillow-komatiite contact in drill core DDH065-W2. (A) A series of merged photographs of a cylindrical drill core. (B) A photo of its opposite cut and polished side. Both photographs are accompanied by sketches highlighting the pillows and other textural features. This drill core is the basal pillowed komatiite unit intersected (see Fig. 2) and its upper part is overlain by spinifex-textured komatiite. The inset in (B) shows an inter-pillow cavity filled by a white talc-carbonate assemblage.

Typeset version here: https://doi.org/10.1016/j.precamres.2020.105729

Figure 4. Thin section of pillowed komatiite. (A) A change in magnetite (black) concentration represents the crust of pillows. Secondary internal crusts (white dashed lines) are also observed. These textures are hypothesized to be evidence for multiple episodes of growth and filling. Blue encircled areas are areas where pseudomorphs after crystals are observed. The white box outlines close-up area shown in (B). (B) Microphotograph showing euhedral and spinifex-textured olivine. The inset is a sketch of that microphotograph highlighting the euhedral olivine (white) and spinifex (black line).

Figure 5. Pillow height and width. Silver Lake komatiite pillows (this study, in green; Table ESM 1) compared with pillow lavas of other compositions from the literature (Table ESM 4). Melt viscosities are computed using the best chemical data available for each locality and therefore serve as best estimates for points of comparison, not exact values. A 300°C temperature variation is shown by the viscosity range; for komatiites the lower temperature is fixed at the liquidus temperature using the equation from Arndt et al. (2008). The range in basalt and andesite pillow sizes represent the 16^{th} and 18^{th} percentile from Walker (1992).

Typeset version here: https://doi.org/10.1016/j.precamres.2020.105729

367 Figure 1

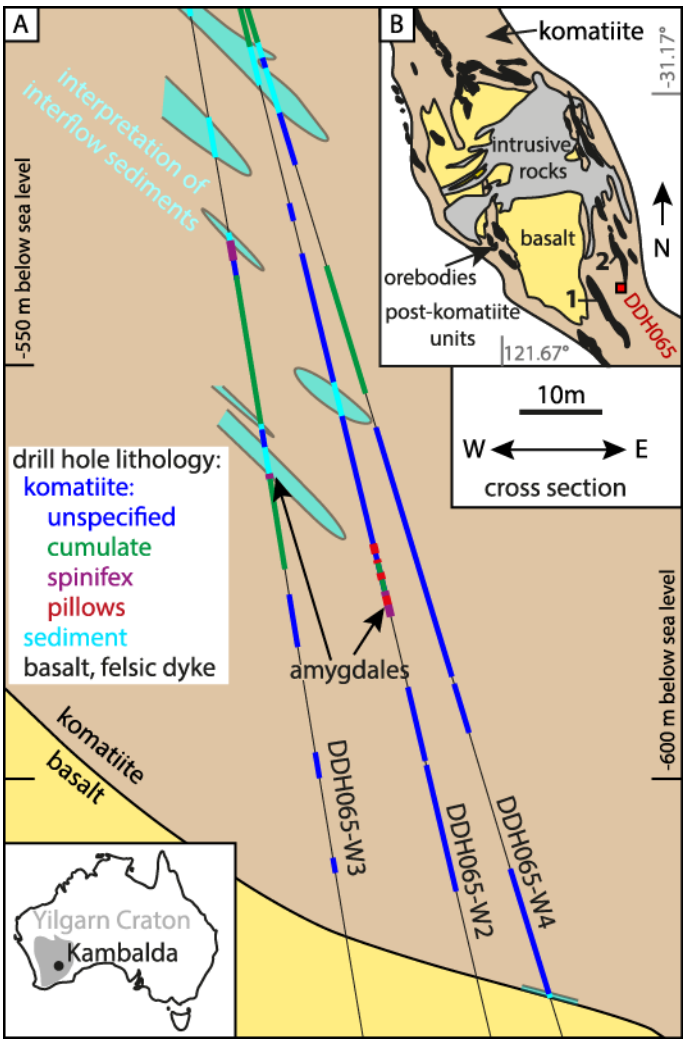

368

369

Typeset version here: https://doi.org/10.1016/j.precamres.2020.105729

370 Figure 2

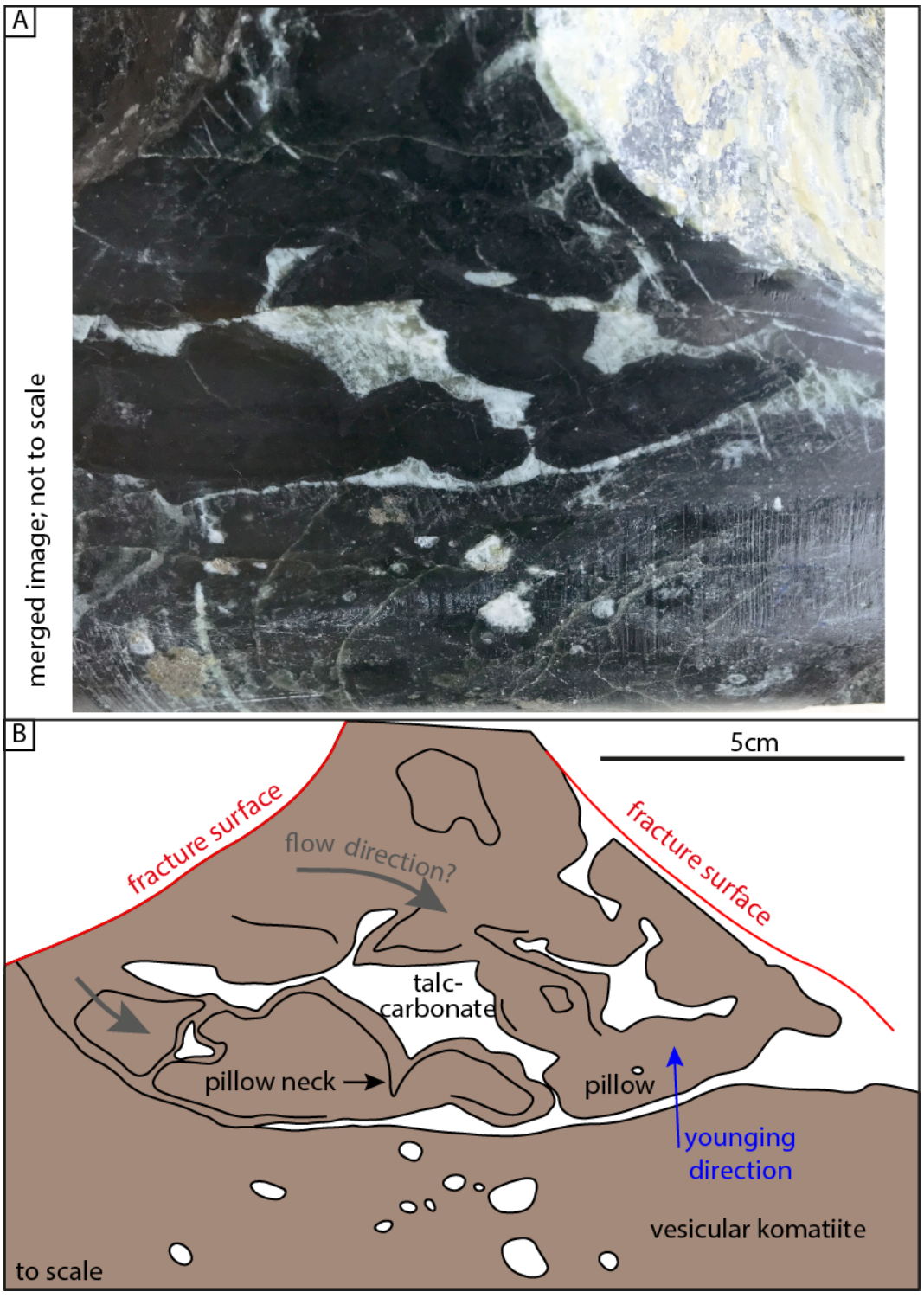

371

372

Typeset version here: https://doi.org/10.1016/j.precamres.2020.105729

373 Figure 3

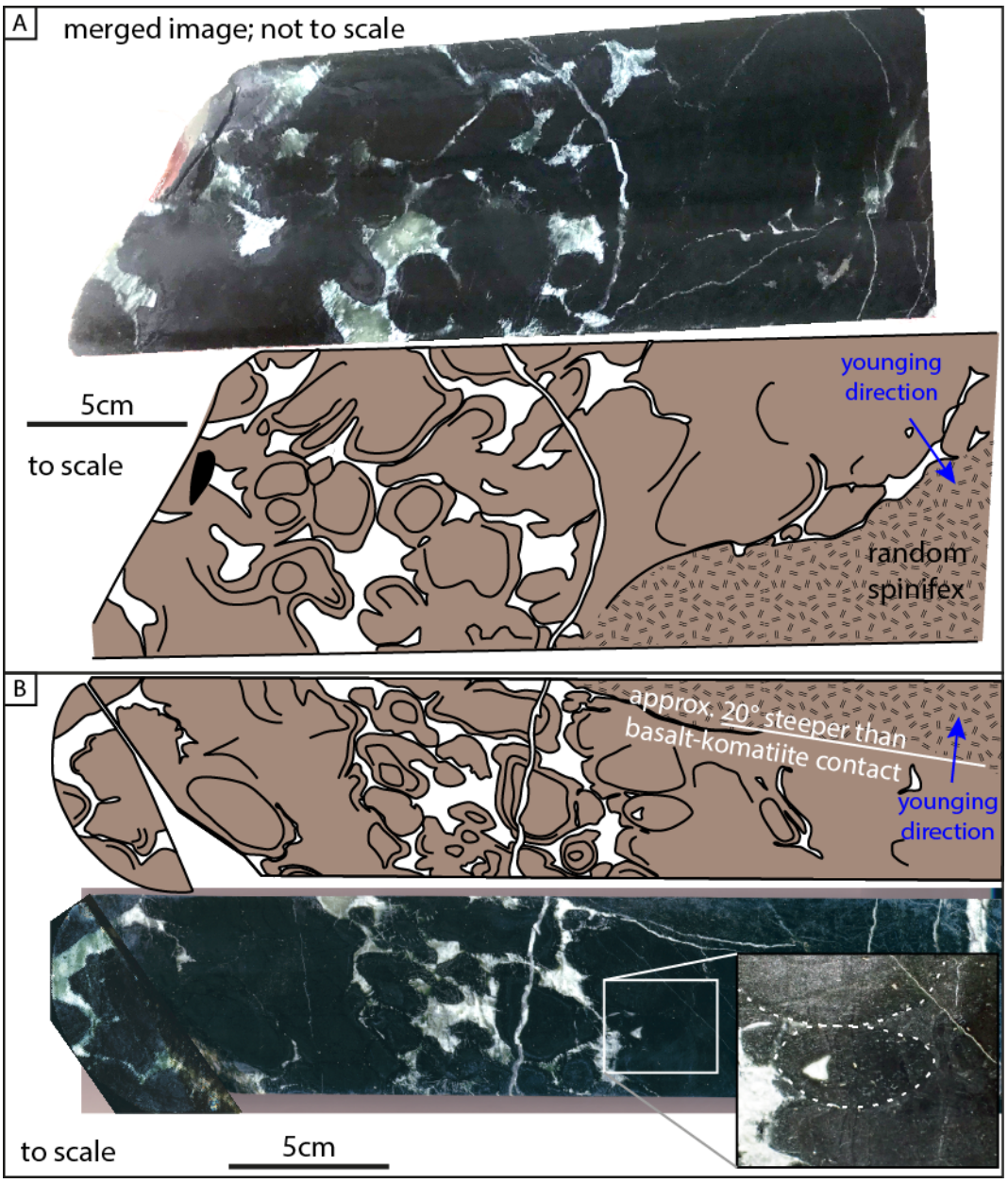

374

375

Typeset version here: https://doi.org/10.1016/j.precamres.2020.105729

376 Figure 4

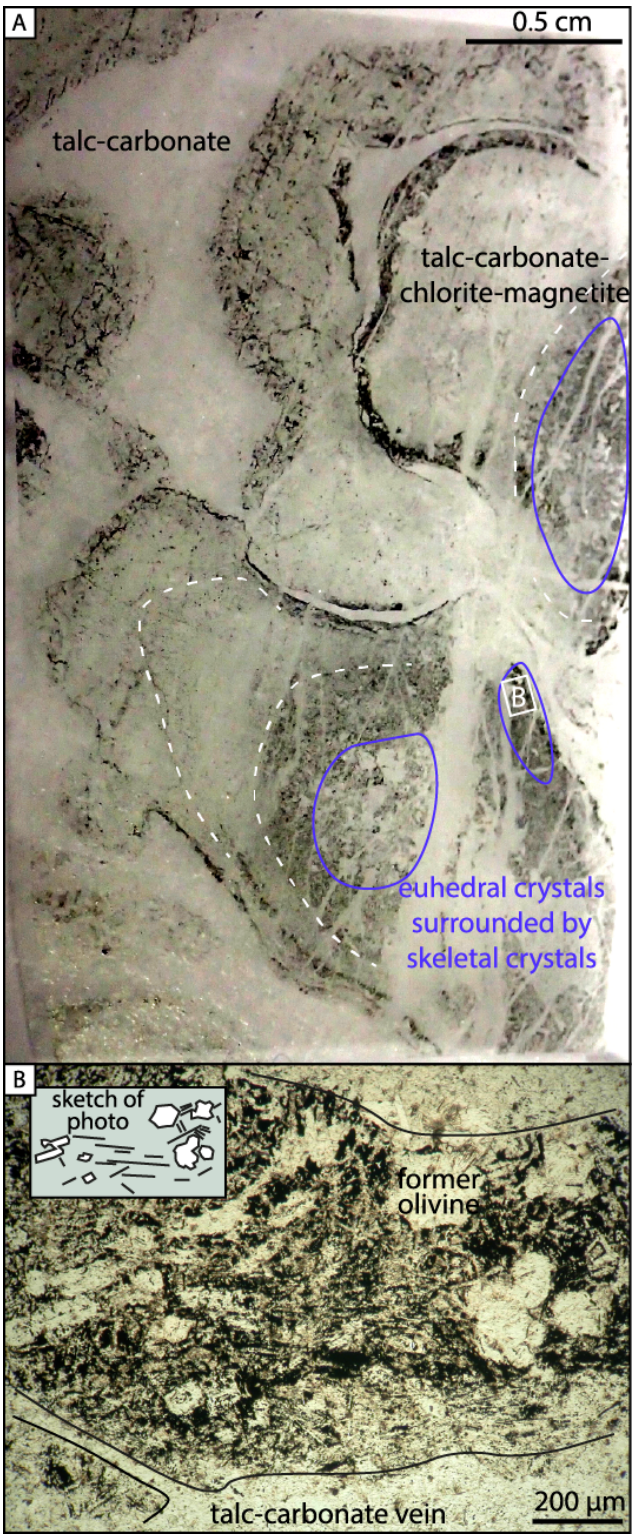

377

378

Typeset version here: https://doi.org/10.1016/j.precamres.2020.105729

379 Figure 5

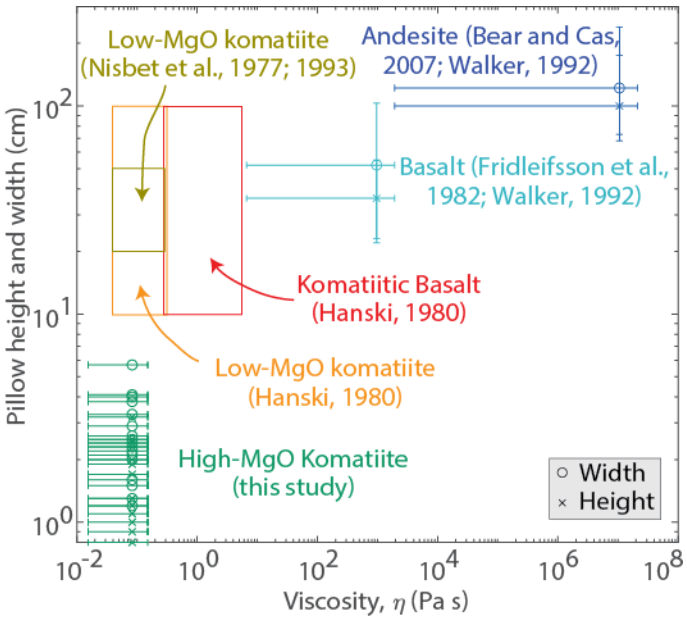

380